ESLAB Seoul National Univ. Nuclear Energy System Lab

2020 KNS Fall

SPH Simulation of Premixed Methane/air Combustion in a Micro-planar Combustor

Jin Woo Kim

Energy System LABoratory
Seoul National University

Contents

Introduction

- **Importance of chemistry in nuclear safety**
  - In HTGR, *gasfication* of graphite structures, which could occur especially during the postulated air-ingress accident, leads to degradation of thermal and mechanical properties of the structures.
  - Zircaloy *oxidation and hydrogen embrittlement* results in a severe loss of ductility and toughness, making the material susceptible to applied stresses.
  - In this study, *homogeneous gas-phase chemical reaction* model has been newly developed in SPH framework and validated.

homogeneous & heterogeneous chemical reaction

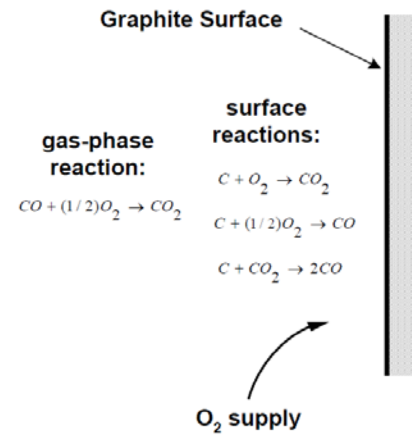

Graphite oxidation (HTGR)

Degradation of core structures

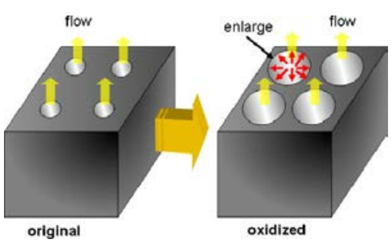

Subchannel enlargement

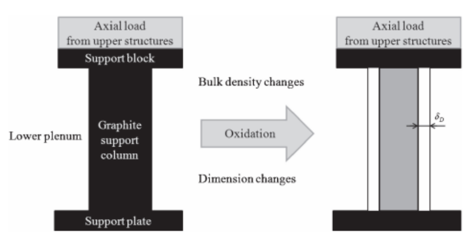

Strength degradation of graphite support column

Zircaloy oxidation & embrittlement

PCT < 1204 ℃
ECR < 17 %

Formation of oxide layer

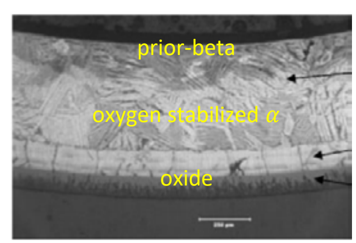

Cladding rupture

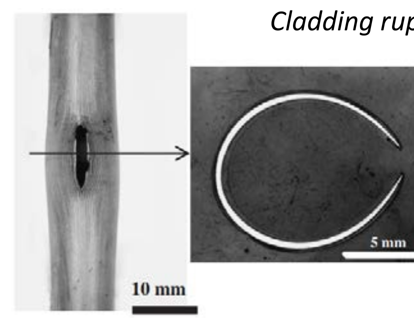

Introduction

- **Premixed methane/air combustion in a micro-planar combustor**

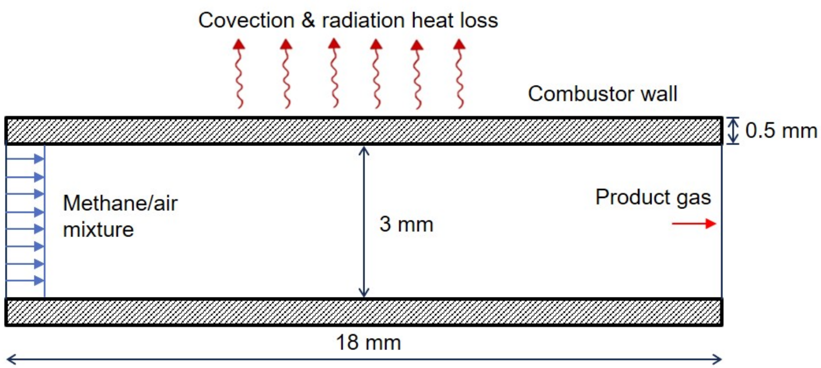

Combustion phenomenon in the combustor

① **Preheating**

- Fresh methane/air mixture injected at the inlet is heated by hot combustor wall.

② **Combustion**

- The heated gas mixture is combusted.

③ **Post-combustion**

- The burned gas flows downstream along the channel and cools down.

BD	Boundary condition
Inlet	• Fixed value: mass fraction, temperature, velocity $Y_{N_2} = 0.725,\ Y_{O_2} = 0.22, Y_{CH_4} = 0.055\ (\Phi = 1.0)$ $T = 300.0\ K, u = 0.4, 0.6\ m/s$
Outlet	• ***Fixed pressure*** & far-field condition for other variables (No energy / species diffusion to the exit)
Wall	• Stainless steel316 • ***Convective & radiative heat transfer***: $h = 15\ W/m^2K, \epsilon = 0.65$ • No slip • No concentration & energy diffusion to the upper & the lower wall

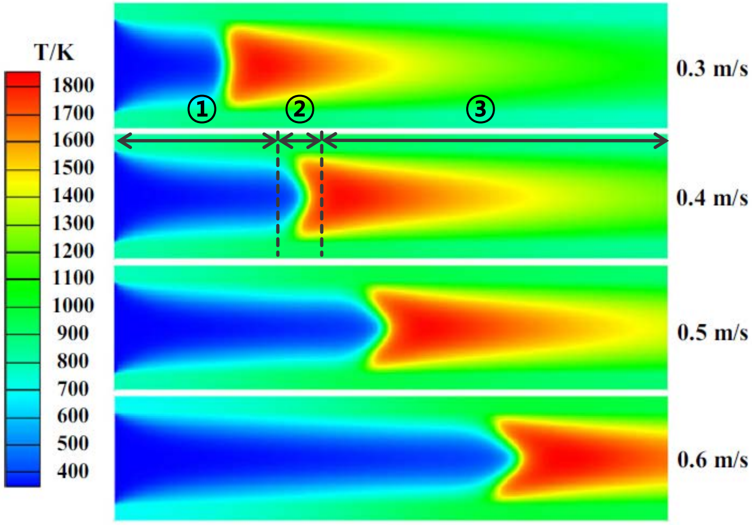

Tang et al.

Introduction

▪ Overview of mathematical models for gas combustion

Author	Fuel-oxidizer	Combustion geometry	Reaction mechanism	Momentum		Energy				
				Pressure	Viscous	Pressure	Viscous	Conduction	Dufour	Reaction
Tang et al.	CH_4 + air	Plane chanel	Detailed gas phase reaction	O	$\frac{\partial \tau_{ij}}{\partial x_j}(\triangle)$	O	O	O	O	O
Norton et al.	CH_4 + air C_3H_8 + air	Parallel plate	One-step global reaction	O	$\frac{\partial \tau_{ij}}{\partial x_j}(\triangle)$	X	X	O	O	O
Chen et al.	CH_4 + air	Parallel plate	One-step global reaction	O	$\frac{\partial \tau_{ij}}{\partial x_j}(\triangle)$	X	X	O	O	O
Li et al.	CH_4 + air H_2 + air	cylindrical tube	Detailed gas phase reaction	O	$\frac{\partial \tau_{ij}}{\partial x_j}$ $(\lambda = -\frac{2}{3}\mu)$	X	X	O	O	O
Niu et al.	CH_4 + air	Parallel plate (bluff body)	Two-step reaction	O	$\frac{\partial \tau_{ij}}{\partial x_j}$ $(\lambda = 0)$	X	X	O	O	O

- Uniform-velocity inlet / pressure outlet boundary condition are imposed in all the bove researches.
- Stress of compressibility is usually considered in all the above researches.
- $\frac{DP}{Dt}$ term in the energy equation is usually neglected.
- Soret effect, which is temperature-gradient-driven diffusion, is neglected in all the above researches.
- Brinkman number tells us that viscous dissipation in the gas combustion can be negligible.

Species diffusion flux $\vec{J}_s = -\rho D_{s,mix}\nabla Y_s - \cancel{D_{s,T}\frac{\nabla T}{T}}$ *Brinkman number* $Br = \frac{\mu u^2}{k\Delta T} = \frac{(1.8e-5)\times 10^2}{0.025\times 2000} = 3.6e-5$

Smoothed Particle Hydrodynamics (SPH)

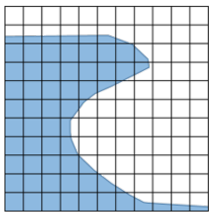

Eulerian

$$\frac{\partial \phi}{\partial t} + u \cdot \nabla \phi$$

Lagrangian

$$\frac{D\phi}{Dt}$$

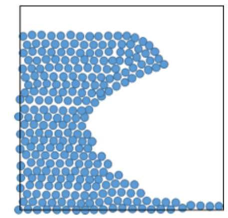

Advantages
① Free surface
② Multi-phase
③ Large deformation
④ Complex geometry

- ***Lagrangian particle-based method*** for simulating the mechanics of continuum media
- Entire system of interest is represented with a set of fluid particles, and its governing equation are solved in discretized form over neighboring particles within a suppor domain.

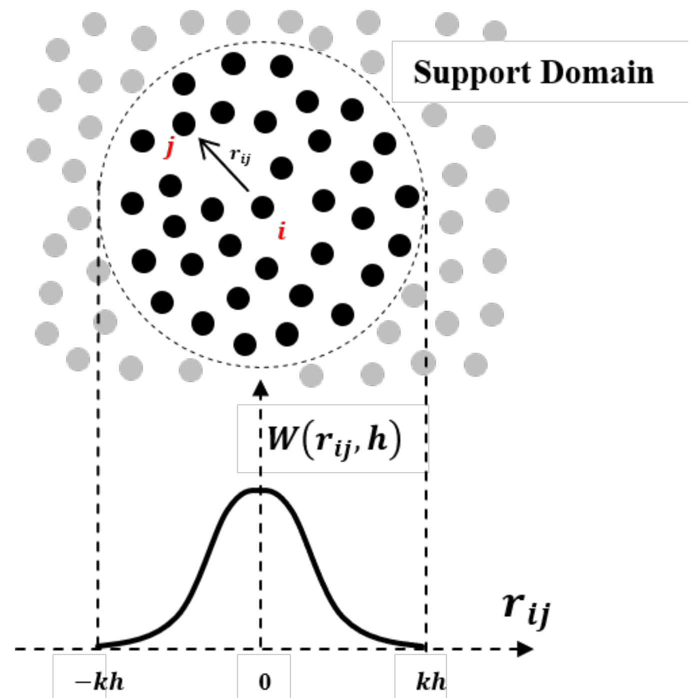

SPH discretization

$$< f >_i = \sum_j f_j W(\vec{r}_i - \vec{r}_j) \frac{m_j}{\rho_j}$$

$$< \nabla f >_i = \rho_i \sum_j m_j \left(\frac{f_i}{\rho_i^2} + \frac{f_j}{\rho_j^2}\right) \nabla_i W_{ij}$$

$$< \nabla^2 f >_i = \sum_j 2 \frac{m_j}{\rho_j} \frac{(f_i - f_j)}{|\vec{r}_{ij}|^2} \vec{r}_{ij} \cdot \nabla_i W_{ij}$$

Smoothed Particle Hydrodynamics (SPH)

- **SOPHIA code**
  - Particle-based SPH solver in SNU for multi-physics flow phenomenon
  - 2D/3D GPU-parallelized code based on CUDA C (nvidia)

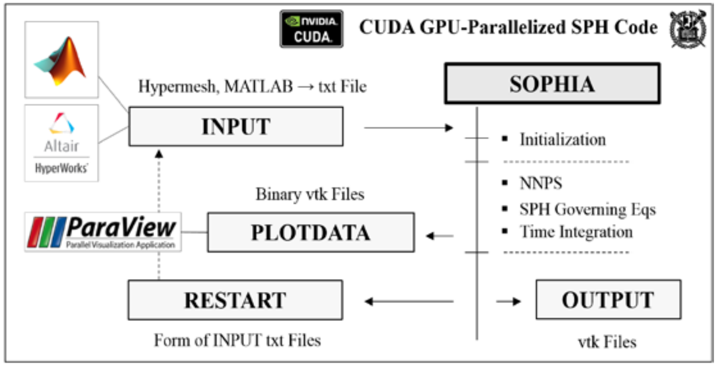

Mathematical models

- **General governing equations for multi-component gas system**

Mass	$\frac{d\rho}{dt} = -\rho\nabla\cdot\vec{u}$	**Momentum**	$\rho\frac{du_j}{dt} = -\frac{\partial P}{\partial x_j} - \frac{\partial}{\partial x_j}\left(\frac{2}{3}\mu\frac{\partial u_k}{\partial x_k}\right) + \frac{\partial}{\partial x_i}\left(\mu\left(\frac{\partial u_i}{\partial x_j} + \frac{\partial u_j}{\partial x_i}\right)\right)$
Species transport	$\frac{d}{dt}\rho Y_k = -\rho Y_k\nabla\cdot\vec{u} + \nabla\cdot(\rho D_{k,m}\nabla Y_k) + \dot{R}_k$	**EOS**	$P = \rho\frac{R}{M}T$
Energy	$\rho c_P\frac{dT}{dt} + \sum_k \rho h_k\frac{dY_k}{dt} = R_T' + \frac{dP}{dt} + \nabla\cdot(k\nabla T) + \sum_{k=1}^{N}\nabla\cdot(h_k\rho D_{k-m}\nabla Y_k)$		

Mathematical models

SPH discretization

✓ General governing equations for multi-component gas system has been newly developed in SPH framework with sufficient numerical accuracy and stabililty.

Mass

$$< \rho >_i = \rho_{ref,i} \sum_j \frac{m_j}{\rho_{ref,j}} W_{ij}$$

EOS

$$P = \rho \frac{R}{M_{mix}} T$$

Species transport

$$< \frac{d}{dt} \rho Y_k >_i = Y_k \frac{\rho_i^n - \rho_i^{n-1}}{\Delta t^n} + \sum_j 2(\rho D_{k-mix})_{ij} \frac{m_j}{\rho_j} (Y_{k,i} - Y_{k,j}) \frac{\vec{r}_{ij} \cdot \nabla_i W_{ij}}{|\vec{r}_{ij}|^2} + \dot{R}_k$$

$$A_{ij} = \frac{2A_i A_j}{A_i + A_j}$$

Momentum

$$< \frac{d\vec{u}}{dt} >_i = \sum_j -m_j \frac{P_i + P_j}{\rho_i \rho_j} L_i \nabla_i W_{ij} + \sum_j 8\mu_{ij} \frac{\vec{r}_{ij} \cdot \vec{u}_{ij}}{|\vec{r}_{ij}|^2} \nabla_i W_{ij} \frac{m_j}{\rho_j} + \sum_j (\lambda_{SPH})_{ij} m_j \left(\frac{< \nabla \cdot \vec{u} >_j^L + < \nabla \cdot \vec{u} >_i^L}{\rho_i \rho_j} \right) L_i \nabla_i W_{ij}$$

Energy

$$\begin{aligned} < \rho c_P \frac{dT}{dt} >_i + \sum_k \rho h_k \frac{Y_k^n - Y_k^{n-1}}{\Delta t^n} &= R_T' + \frac{P_i^n - P_i^{n-1}}{\Delta t_n} + \sum_j 2k_{ij} \frac{m_j}{\rho_j} (T_i - T_j) \frac{\vec{r}_{ij} \cdot \nabla_i W_{ij}}{|\vec{r}_{ij}|^2} \\ &+ \sum_k \sum_j 2(\rho h_k D_{k-mix})_{ij} \frac{m_j}{\rho_j} (Y_{k,i} - Y_{k,j}) \frac{\vec{r}_{ij} \cdot \nabla_i W_{ij}}{|\vec{r}_{ij}|^2} \end{aligned}$$

Mathematical models

- **SPH discretization**

  ✓ General governing equations for multi-component gas system has been newly developed in SPH framework with sufficient numerical accuracy and stabililty.

Mass

$$< \rho >_i = \rho_{ref,i} \sum_j \frac{m_j}{\rho_{ref,j}} W_{ij}$$

EOS

$$P = \rho \frac{R}{M_{mix}} T$$

Species transport

$$< \frac{d}{dt}\rho Y_k >_i = Y_k \frac{\rho_i^n - \rho_i^{n-1}}{\Delta t^n} + \sum_j 2(\rho D_{k-mix})_{ij} \frac{m_j}{\rho_j} (Y_{k,i} - Y_{k,j}) \frac{\vec{r}_{ij} \cdot \nabla_i W_{ij}}{|\vec{r}_{ij}|^2} + \dot{R}_k$$

$$A_{ij} = \frac{2A_i A_j}{A_i + A_j}$$

Momentum

$$< \frac{d\vec{u}}{dt} >_i = \sum_j -m_j \frac{P_i + P_j}{\rho_i \rho_j} L_i \nabla_i W_{ij} + \sum_j 8\mu_{ij} \frac{\vec{r}_{ij} \cdot \vec{u}_{ij}}{|\vec{r}_{ij}|^2} \nabla_i W_{ij} \frac{m_j}{\rho_j} + \sum_j (\lambda_{SPH})_{ij} m_j \left(\frac{< \nabla \cdot \vec{u} >_j^L + < \nabla \cdot \vec{u} >_i^L}{\rho_i \rho_j} \right) L_i \nabla_i W_{ij}$$

Energy

$$< \rho c_P \frac{dT}{dt} >_i + \sum_k \rho h_k \frac{Y_k^n - Y_k^{n-1}}{\Delta t^n} = R_T' + \frac{P_i^n - P_i^{n-1}}{\Delta t_n} + \sum_j 2k_{ij} \frac{m_j}{\rho_j} (T_i - T_j) \frac{\vec{r}_{ij} \cdot \nabla_i W_{ij}}{|\vec{r}_{ij}|^2} + \sum_k \sum_j 2(\rho h_k D_{k-mix})_{ij} \frac{m_j}{\rho_j} (Y_{k,i} - Y_{k,j}) \frac{\vec{r}_{ij} \cdot \nabla_i W_{ij}}{|\vec{r}_{ij}|^2}$$

One-step global reaction
(Westbook & Dryer)

Chemical kinetics

$$\dot{R}_{CH_4} = 6.7e+9 \exp\left(-\frac{202505.6}{RT} \right) [CH_4]^{0.2} [O_2]^{1.3}$$

Mathematical models

- **Thermal properties**

	Pure gas	Gas mixture
Specific heat	$c_P^o = A + Bt + Ct^2 + Dt^3 + \frac{E}{t^2}$	$c_{p,mix} = \sum_i Y_i c_{p,i}$
Enthalpy	$h^o - h_{298.15}^o = At + \frac{Bt^2}{2} + \frac{Ct^3}{3} + \frac{Dt^4}{4} - \frac{E}{t} + F - H$	$h_{mix} = \sum_i Y_i h_i$
Viscosity	$\mu_i = 2.669 \times 10^{-6} \frac{(M_i T)^{0.5}}{\sigma_i^2 \Omega_v}$	$\mu_{mix} = \sum_i Y_i \mu_i$
Diffusivity	$D_{ab} = \frac{0.00266 T^{3/2}}{P \sigma_{ab}^2 M_{ab}^{0.5} \Omega_D}$	$D_{s-mix} = \frac{1 - f_s}{\sum_{j,j \neq s}(f_j / D_{sj})}$
Conductivity	$k_i = \frac{15}{4} \frac{R}{M_{mix,i}} \mu_i \left[\frac{4}{15} \frac{c_{p,i} M_{mix,i}}{R} + \frac{1}{3} \right]$	$k_{mix} = \sum_i Y_i k_i$

SPH numerical shemes

- **SPH open boundary model**
  - SPH open boundary model is employed to simulate a simple planar channel flow.
  - SOPHIA has been successfully solved numerous hydrodynamic phenomenon in channel flows as below.

Simulation input in this study

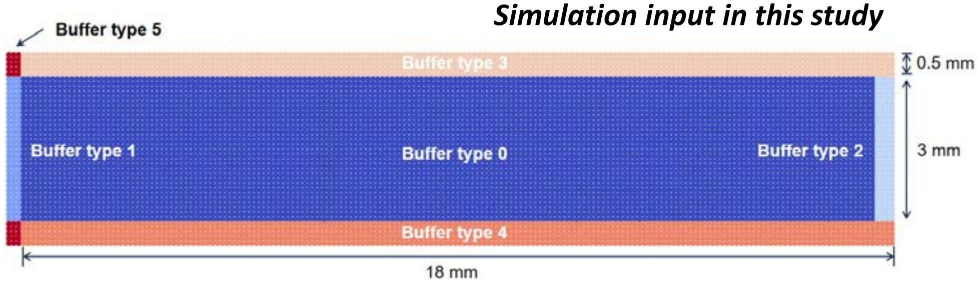

Buffer type 1	*Inlet*
Buffer type 2	*Outlet*
Buffer type 3/4	*Wall*
Buffer type 5	*Dummy*

Velocity field

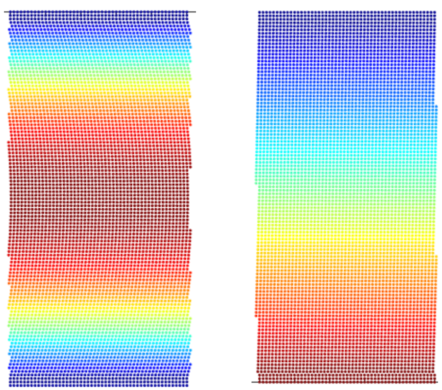

Poiseuille flow ***Couette flow***

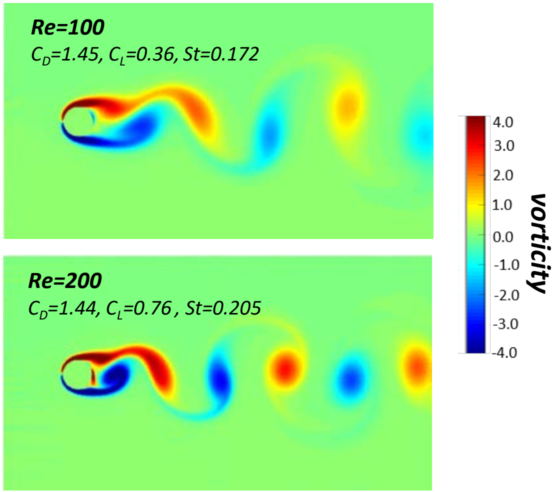

Karman vortex street

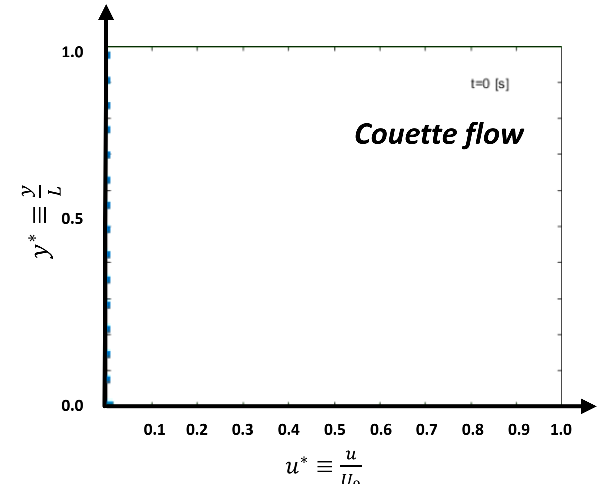

SPH numerical shemes

▪ SPH open boundary model

- ➢ SPH open boundary model is employed to simulate a simple planar channel flow.
- ➢ SOPHIA has been successfully solved numerous hydrodynamic phenomenon in channel flows as below.

Simulation input in this study

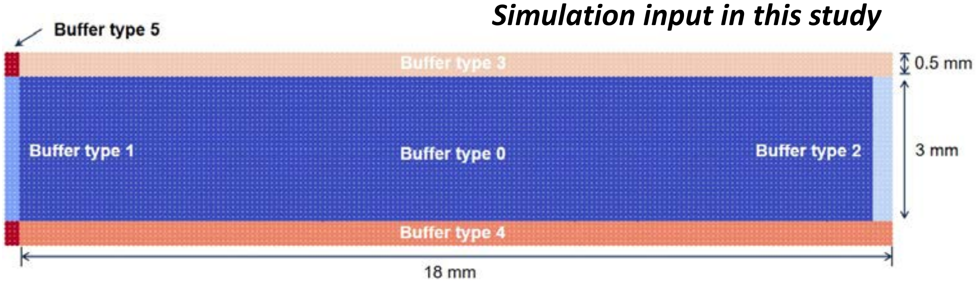

Buffer type 1	*Inlet*
Buffer type 2	*Outlet*
Buffer type 3/4	*Wall*
Buffer type 5	*Dummy*

Velocity field

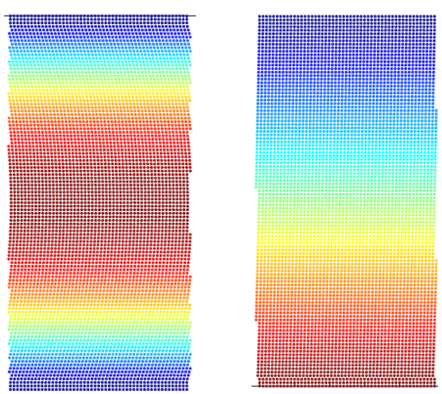

Poiseuille flow ***Couette flow***

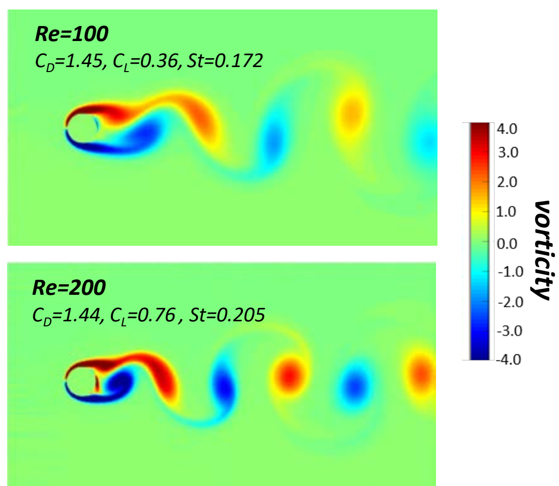

Karman vortex street

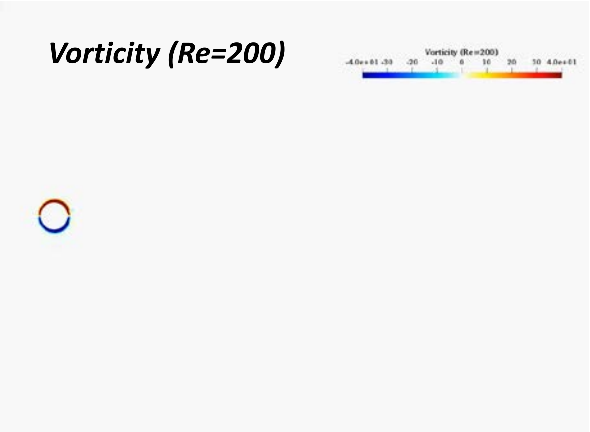

SPH numerical shemes

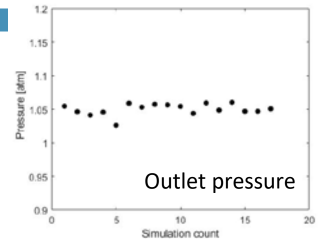

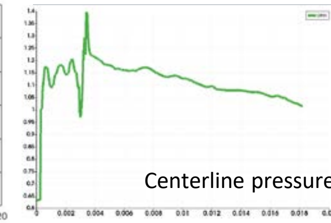

▪ SPH pressure-outlet boundary model

- To satisfy *fixed-pressure condition (1atm)* at the outlet, SPH pressure outlet boundary model has been newly constructed.

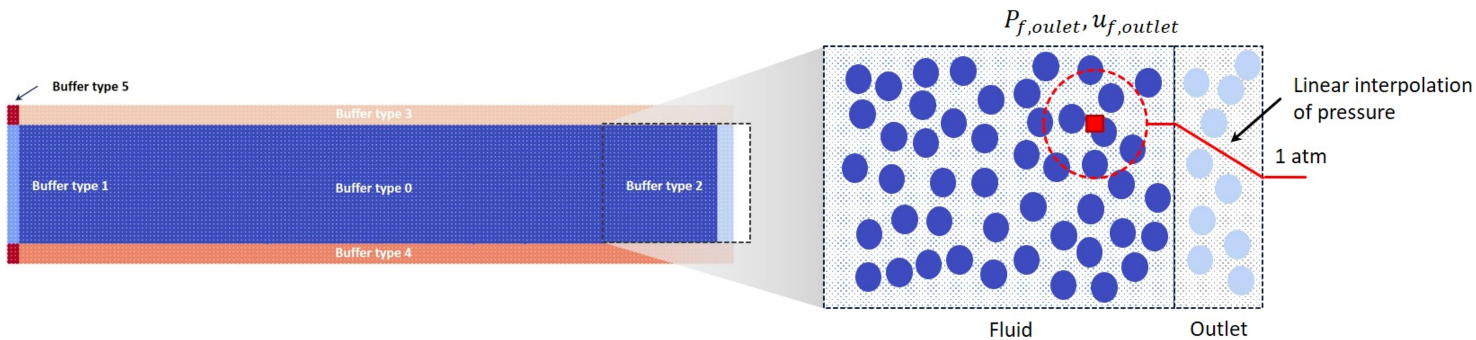

- The linear interpolation of pressure is imposed on outlet buffer particles and the momentum of gas particles near the outlet is greatly affected by the linear pressure distribution.
- With the linear pressure distribution, flames tend to be blown out of the exit without any treatments with $P_{f,outlet}$ below 1 atm. The following is its treatment.

This condition leads to

$$P_{f,outlet} < 1.02\ atm \longrightarrow u_{outlet} = \beta \frac{\rho_{inlet}}{\rho_{outlet}} u_{inlet} \quad (\beta = 0.6 \sim 0.8)$$

Density ↑

$$Otherwise \longrightarrow u_{outlet} = u_{f,outlet}$$

SPH numerical shemes

▪ Adaptive particle splitting model (Liu and Sun)

- Fresh methane/air mixture expands its volume drastically due to the wall heating and the combustion, leading to low accuracy of SPH interpolation. To address the problem, APS model is applied.
- To prevent *pairing instability* due to large smoothing length compared to particle size, the artificial pressure-like function (Monaghan) is employed with slight reformation.

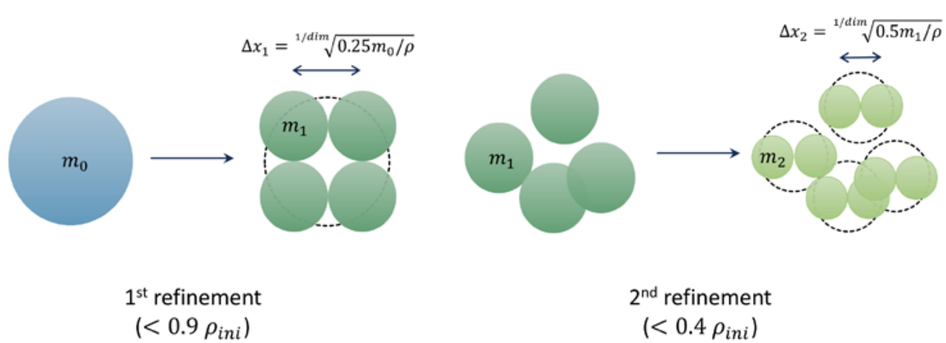

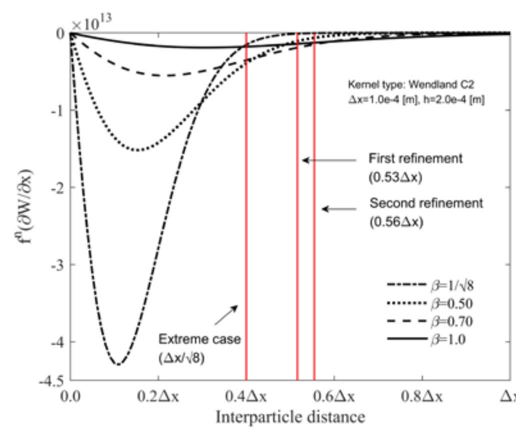

Constant smoothing length ⟶ Minimum splitting error

$$< \frac{d\vec{u}}{dt} >_i^{fp} = \sum_j -m_j\left(\frac{P_i + P_j}{\rho_i \rho_j} \nabla_i W_{ij} + R f^n \nabla_i W_{ij}^{\beta}\right)$$

$$R \equiv \epsilon\left(\frac{P_i + P_j}{\rho_i \rho_j}\right), n = 4, \beta = 0.5\left(\sqrt{m_i/\rho_i} + \sqrt{m_j/\rho_j}\right), f \equiv \frac{W(\vec{r}_{ij}, \beta h_i)}{W(\beta \Delta x, \beta h_i)}, \nabla_i W_{ij}^{\beta} = \nabla_i W(\vec{r}_{ij}, \beta h_i)$$

typical value of $\epsilon = 0.2$ ($\epsilon = 0.001$ in this study)

SPH numerical shemes

- **SPH thermal boundary model**
  - SPH <u>convective & radiative</u> thermal boundary (Fraser et al.)

Morris-type Laplacian model
- known to have high accuracy
- not sensitive to particle disorder
- captures sptial variance of k well

Morris-type

$$< \rho c_P \frac{dT}{dt} >_i = \sum_j \frac{4k_i k_j}{k_i + k_j} \frac{m_j}{\rho_j} (T_i - T_j) \frac{\vec{r}_{ij} \cdot \nabla_i W_{ij}}{|\vec{r}_{ij}|^2} + \frac{h_{conv,i}(T_{sur} - T_i)}{\Delta x} + \frac{\epsilon_i \sigma_{SB} (T_{sur}^4 - T_i^4)}{\Delta \mathrm{x}}$$

$$where\ i \in \Omega_{suface}, \Delta x: particle\ size$$

  - Simple validation: comparison with 1D-FDM results

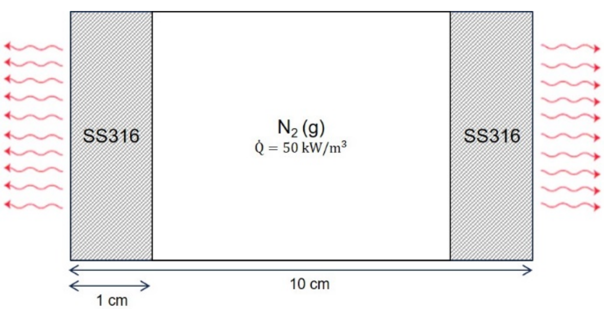

Simulation geometry

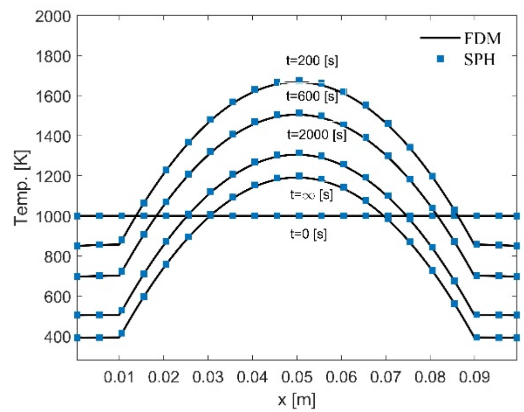

SPH vs. FDM

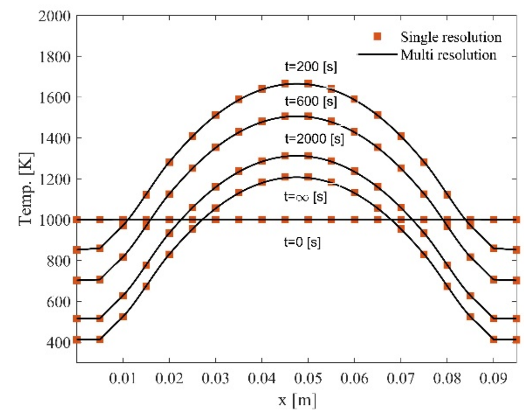

SPH single vs. multi-resolution

SPH numerical shemes

▪ SPH thermal boundary model

- SPH convective & radiative thermal boundary (Fraser et al.)

$$< \rho c_P \frac{dT}{dt} >_i = \sum_j \frac{4k_i k_j}{k_i + k_j} \frac{m_j}{\rho_j} (T_i - T_j) \frac{\vec{r}_{ij} \cdot \nabla_i W_{ij}}{|\vec{r}_{ij}|^2} + h_i$$

$$where\ i \in \Omega_{suface}, \Delta x: part$$

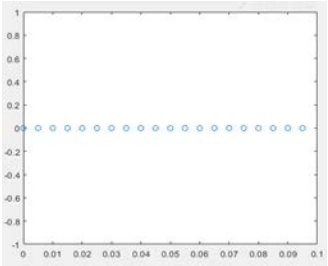

Single resolution

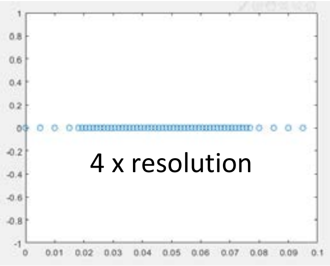

Multi-resolution

- Simple validation: comparison with 1D-FDM results

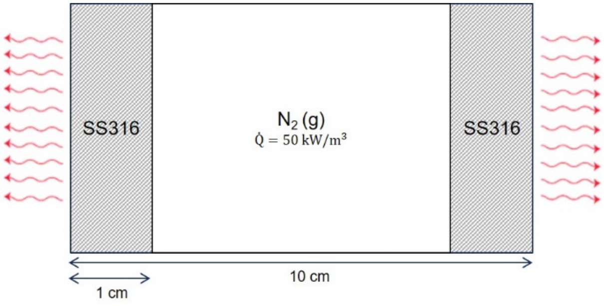

Simulation geometry

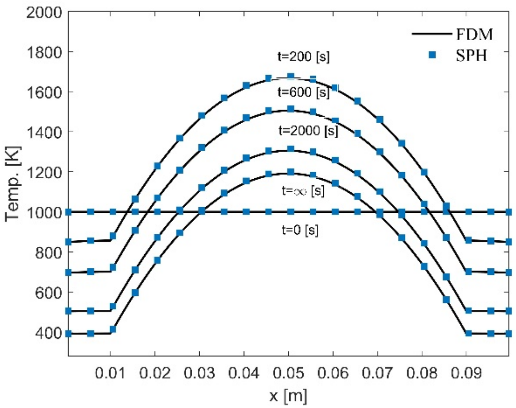

SPH vs. FDM

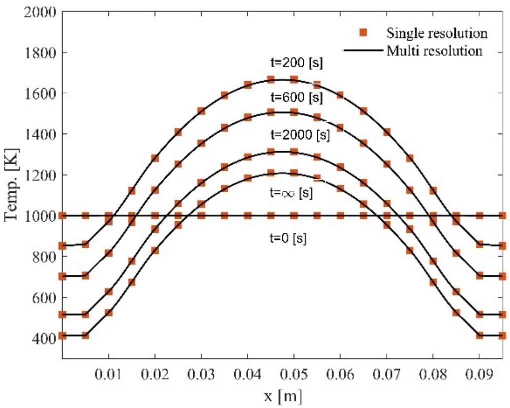

SPH single vs. multi-resolution

Simulation setup

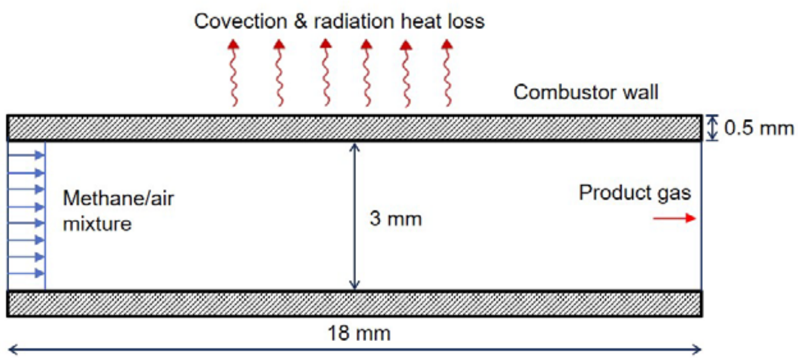

Simulation geometry

SPH numerical scheme

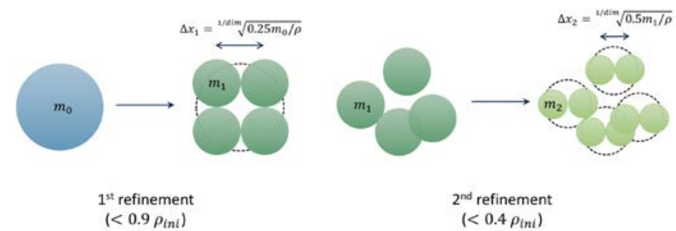

Particle splitting

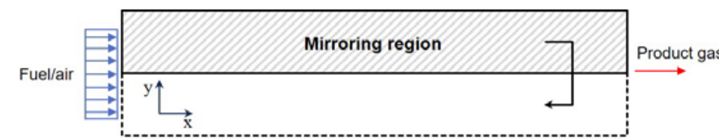

Open & symmetric boundary

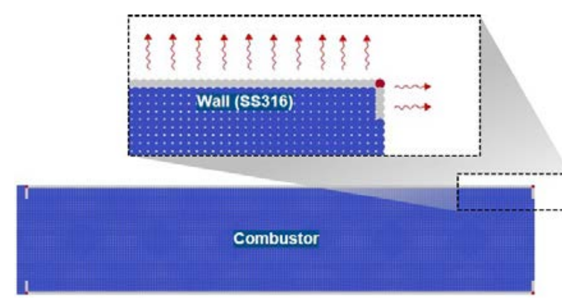

Convective & radiative heat loss

Boundary conditions

BD	Boundary condition
Inlet	• Fixed value: mass fraction, temperature, velocity $Y_{N_2} = 0.725,\ Y_{O_2} = 0.22, Y_{CH_4} = 0.055\ (\Phi = 1.0)$ $T = 300.0\ K, u = 0.4, 0.6\ m/s$
Outlet	• ***Fixed pressure*** & far-field condition for other variables (No energy / species diffusion to the exit)
Wall	• Stainless steel316 • ***Convective & radiative heat transfer***: $h = 15\ W/m^2K, \epsilon = 0.65$ • No slip • No concentration & energy diffusion to the upper & the lower wall

Results and discussion

Flame structure

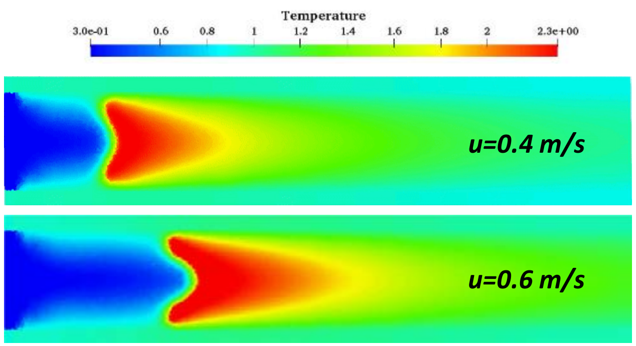

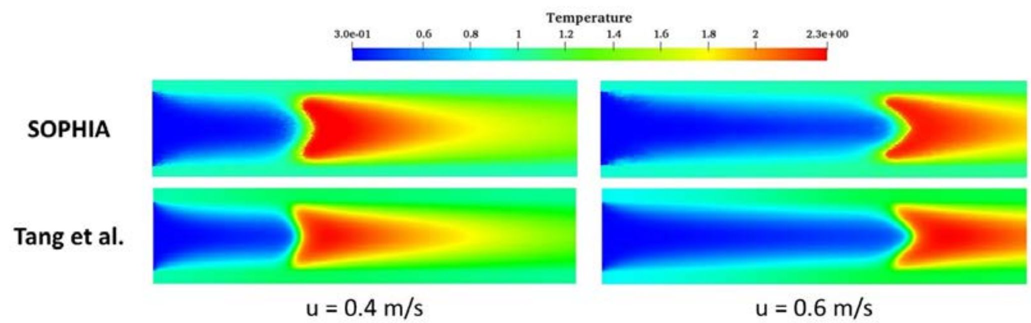

Wall temperature distribustion

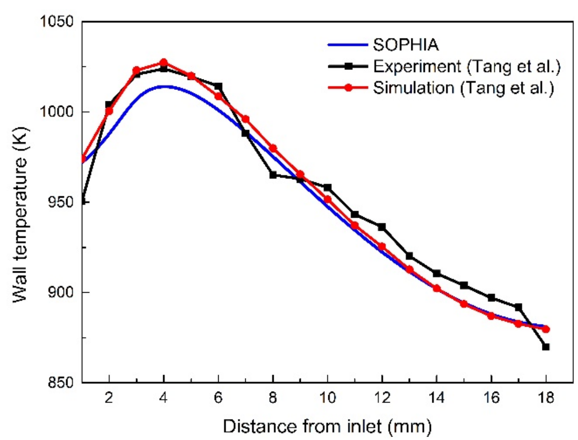

u=0.4 m/s

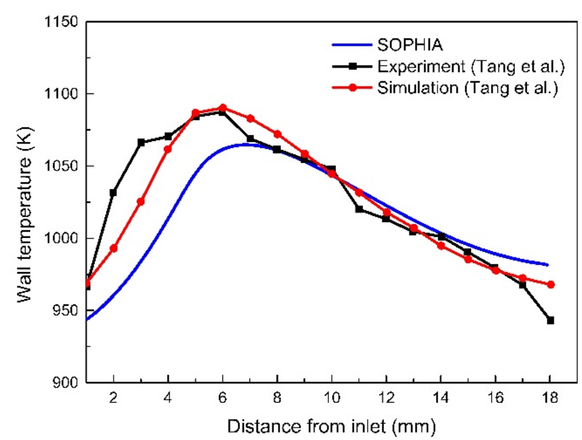

u=0.6 m/s

Conclusion

I. Development of gas-phase chemical model in SPH methodology

- Gas-phase chemical reaction model, which is based on ***Arrhenius equation***, has been constructed in SPH framework and implemented into SOPHIA code.
- The effect of chemical reaction on ***species transport equation*** was considered, coupled with ***molecular diffusion***. Enthalpy of chemical reaction and energy transport by the diffusion (Dufour effect) were newly added into ***energy equation***, assuring sufficient sufficient numerical accuracy even in particle disorder.

II. Model validation

- For validation of the chemical reaction model, simulation of ***premixed methane/air combustion*** in a micro-planar combustor is carried out with the additional SPH numerical schemes, comparing results with the benchmark experiments and simulations.
- SOPHIA obtained the ***similar flame structure and location*** with Tang et al for both cases of u=0.4, 0.6 m/s
- SOPHIA also gave very good agreements with Tang et al. in terms of the ***wall temperature distribution***, having maximum error about 3.0%.

Appendix A

- **Chemical kinetics**

$CH_4 + 2(O_2 + 3.76N_2) \rightarrow CO_2 + 2H_2O + 7.52N_2$ -802.6 kJ/mol

- Combustion mechansism used in this study is a **one-step irreversible reaction** by Westbook & Dryer.

$$\dot{R}_{CH_4} = 6.7e+9\exp\left(-\frac{202505.6}{\bar{R}T}\right)[CH_4]^{0.2}[O_2]^{1.3}$$ **Westbook & Dryer**

$$\dot{R}^n_{CH_4}\Delta t^n \le min([CH_4]^n, [O_2]^n)$$

- Chemical reaction of a gas particle is modeled to occur only within it, and is affected by its adjacent particles through molecular diffusion process.

This simplified mechanism gives quite reasonable results with the detailed one!

Chen et al.

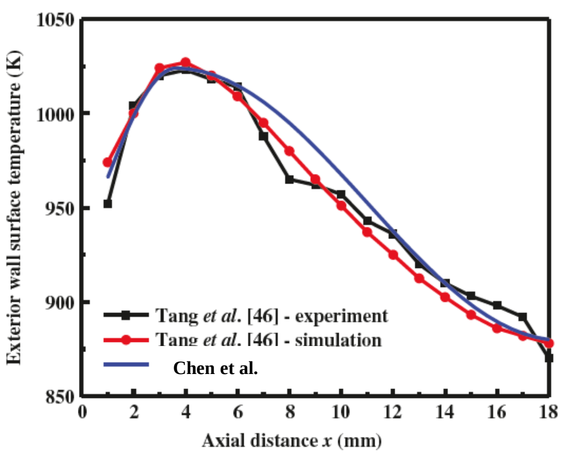

(a)

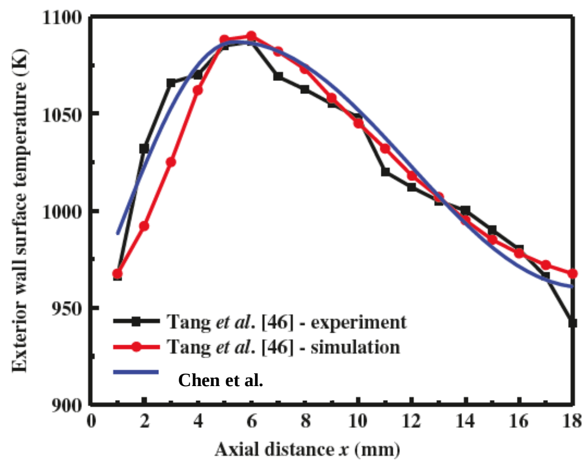

(b)

Tang et al.	Chen et al.
Detailed reaction mechanism	One-step irreversible reaction
16 species, 25 reversible reactions	5 species, single irreversible reaction
3 dimension	2 dimension

Appendix B

- **Viscous stress with compressible effect**

$$\frac{D\rho}{Dt} = -\rho\nabla\cdot\vec{v} \neq 0 \rightarrow$$ **Compressible effect is not negligible!**

Stress tensor $\rho\frac{d\vec{u}}{dt} = \nabla\cdot\bar{\boldsymbol{\tau}}$

$$\bar{\boldsymbol{\tau}} = \begin{pmatrix} \boxed{-P + 2\mu\frac{\partial u}{\partial x} + \lambda\nabla\cdot\vec{u}} & \mu\left(\frac{\partial u}{\partial y} + \frac{\partial v}{\partial x}\right) & \mu\left(\frac{\partial u}{\partial z} + \frac{\partial w}{\partial x}\right) \\ \mu\left(\frac{\partial u}{\partial y} + \frac{\partial v}{\partial x}\right) & \boxed{-P + 2\mu\frac{\partial v}{\partial y} + \lambda\nabla\cdot\vec{u}} & \mu\left(\frac{\partial v}{\partial z} + \frac{\partial w}{\partial y}\right) \\ \mu\left(\frac{\partial u}{\partial z} + \frac{\partial w}{\partial x}\right) & \mu\left(\frac{\partial v}{\partial z} + \frac{\partial w}{\partial y}\right) & \boxed{-P + 2\mu\frac{\partial w}{\partial z} + \lambda\nabla\cdot\vec{u}} \end{pmatrix}$$

Invariant of stress tensor

Mechanical pressure

$$\frac{1}{3}\tau_{ii} = -\bar{P} = -P + \left(\frac{2\mu}{3} + \lambda\right)\nabla\cdot\vec{u}$$

Second viscosity

$$-\bar{P} + P = \left(\frac{2\mu}{3} + \lambda\right)\nabla\cdot\vec{u} = 0$$

Stokes hypothesis

$$\kappa = \left(\frac{2\mu}{3} + \lambda\right) = 0$$

μ: dynamic viscosity
λ: second viscosity
κ: bulk viscosity
n: spatial dimension

Viscous model of Monaghan and Gingold

$$\vec{F}_v^{MG} = (2n+2)\sum_j \frac{2\mu_i\mu_j}{\mu_i + \mu_j}\frac{\vec{r}_{ij}\cdot\vec{v}_{ij}}{|\vec{r}_{ij}|^2}\nabla_i W_{ij}\frac{m_j}{\rho_j}$$

$$\lim_{h\to 0}\vec{F}_v^{MG} = \mu\nabla^2\vec{u} + 2\mu\nabla(\nabla\cdot\vec{u})$$ Colagrossi et al. (2011)

Physical viscous force

$$\vec{F}_v = \mu\nabla^2\vec{u} + (\lambda + \mu)\nabla(\nabla\cdot\vec{u})$$

➢ MG viscous model implies $\lambda = \mu$ (shear-viscosity-dependent bulk viscosity).

Appendix B

- **Viscous stress with compressible effect**

  - MG viscous model implies $\lambda = \mu$ (shear-viscosity-dependent bulk viscosity).
  - Bonet et al. (2020) proposed **shear-viscosity-independent** bulk-viscosity term from MG viscous model.

Physical viscous force $\vec{F}_v = \boxed{\mu\nabla^2\vec{u} + (\lambda+\mu)\nabla(\nabla\cdot\vec{u})}$

$$\vec{f}_v = \vec{F}_v^{MG} + \lambda_{SPH}\nabla(\nabla\cdot\vec{u}) = \boxed{\boxed{\mu\nabla^2\vec{u} + 2\mu\nabla(\nabla\cdot\vec{u})} + \boxed{\lambda_{SPH}\nabla(\nabla\cdot\vec{u})}} \qquad \lambda_{SPH} = \lambda - \mu = \kappa - \frac{5}{3}\mu$$

$$\vec{f}_v = \boxed{(2n+4)\sum_j \mu_{ij}\frac{\vec{r}_{ij}\cdot\vec{u}_{ij}}{|\vec{r}_{ij}|^2}\nabla_i W_{ij}\frac{m_j}{\rho_j}} + \boxed{\sum_j (\lambda_{SPH})_{ij} m_j \left(\frac{<\nabla\cdot\vec{u}>_j + <\nabla\cdot\vec{u}>_i}{\rho_j}\right)\nabla_i W_{ij}}$$

$$\Phi = (n+2)\sum_j \mu_{ij}\frac{\vec{r}_{ij}\cdot\vec{u}_{ij}}{|\vec{r}_{ij}|^2}\vec{u}_{ji}\cdot\nabla_i W_{ij}\frac{m_j}{\rho_j} + \sum_j 0.5(\lambda_{SPH})_{ij} m_j \left(\frac{<\nabla\cdot\vec{u}>_j + <\nabla\cdot\vec{u}>_i}{\rho_j}\right)\vec{u}_{ji}\cdot\nabla_i W_{ij}\frac{m_j}{\rho_j}$$

Brinkman number $Br = \dfrac{\mu u^2}{k\Delta T} = \dfrac{(1.8e-5)\times 10^2}{0.025\times 2000} = 3.6e-5 \ll 1 \sim \dfrac{viscous\ heating}{conduction}$

Appendix C

▪ Equation of state: ideal gas law

$$P_i = \rho_i \bar{R}_i T_i$$

R: universal gas constant
$\bar{R}$: specific gas constant
$\bar{R} = R/M_{mix}$

- Gas has low inertia and high pressure compared to liquids, resulting in large acceleration. Thus, SPH gas simulation needs very fine time-step.

$$\left(\frac{d\vec{u}}{dt}\right)_P = -\frac{1}{\rho}\nabla P \sim \frac{high\ pressure}{low\ inertia}$$

- When adopting ideal gas law, it may be reasonable to select artificial speed of sound like Tait's equation for numerical stability.

$Ma \equiv \frac{u_{max}}{c} \sim 0.1$ for incompressibility

$$c = \sqrt{\left(\frac{\partial P}{\partial \rho}\right)_s} = \sqrt{\gamma \bar{R} T} \qquad c_{sim} = \frac{u_{max}}{Ma} = \sqrt{\gamma \bar{R}' T}$$

$$\frac{\bar{R}'}{\bar{R}} = \left(\frac{u_{max}}{Ma}\right)^2 \left(\frac{1}{\gamma \bar{R} T}\right) = \left(\frac{u_{max}}{Ma}\right)^2 \left(\frac{M_{mix}}{\gamma R T}\right)$$

$$\therefore P = \rho \bar{R} T \times \left(\frac{\bar{R}'}{\bar{R}}\right) = \rho \bar{R}' T$$

In code

$$\left(\frac{d\vec{u}}{dt}\right)_{pres} = -\frac{1}{\rho}\nabla P \times \left(\frac{\bar{R}'}{\bar{R}}\right)$$

$$\left(\rho c_p \frac{dT}{dt}\right)_{pres} = \frac{dP}{dt} \times \left(\frac{\bar{R}'}{\bar{R}}\right)$$

$\bar{R}$: real specific gas constant
$\bar{R}'$: artificial specific gas constant

$\left(\frac{\bar{R}'}{\bar{R}}\right) \sim O(10^{-3})$

Appendix D

- **Numerical accuracy of particle splitting model**

particle splitting

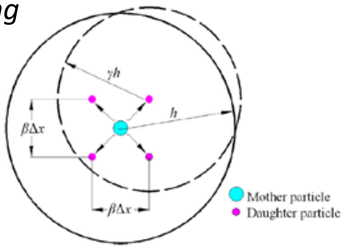

$$\gamma \equiv \frac{h_{daughter}}{h_{mother}}$$

Gradient error of particle splitting

$$e_{\Omega}(r_i) = \sum_{i \neq n} e^{\nabla W}(\vec{r}_i, \vec{r}_n) \frac{m_n}{\rho_n} \text{ where } e^{\nabla W}(\vec{r}_i, \vec{r}_n) = \left[\nabla_i W_{in}(\vec{r}_{in}, h_{in}) - \sum_{k=1}^{4} 0.25 \nabla_i W(\vec{r}_{ik}, h_{ik}) \right]^2$$

- $e^{\nabla W}(\vec{r}_i, \vec{r}_n)$: error of particle *i* when a single particle *n* is split in a support domain of particle *i*
- $e_{\Omega}(r_i)$: error of particle *i* when all particles (particle *n*) in the neighborhood are split.
- Error of particle splitting is exponentially decreased as γ approaches to unity.

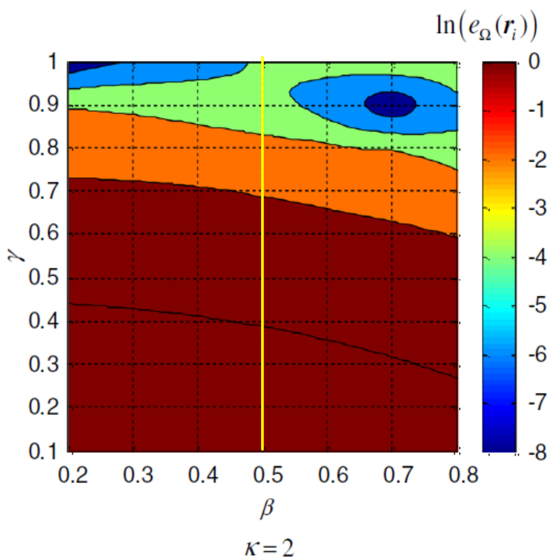

Numerical Test: Hydrostatic pressure

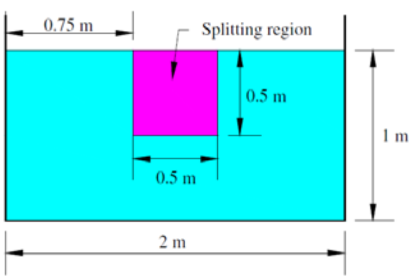

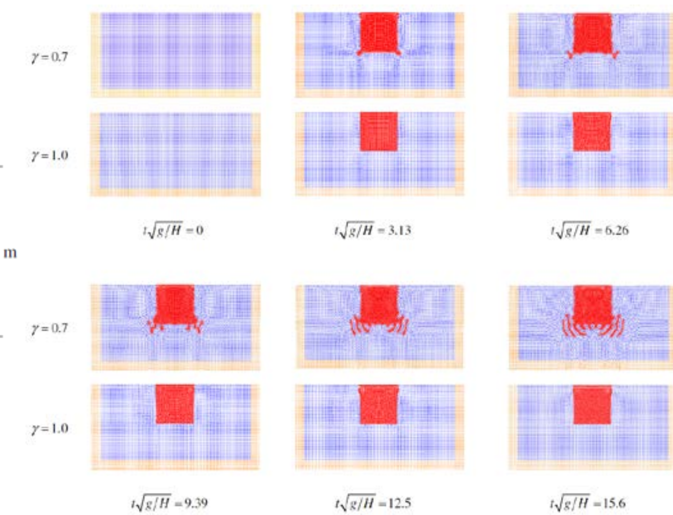

Appendix E

▪ Symmetric boundary

- Non-physical asymmetric flame structures are observed without any treatments. We suspect that this is due to round-off errors in computing operations on GPUs.
- Symmetric boundary model, which simply mirrors the top half of the system with all flow field variables being symmetrized about x-axis, was newly constructed to satisfy the symmetry condition.

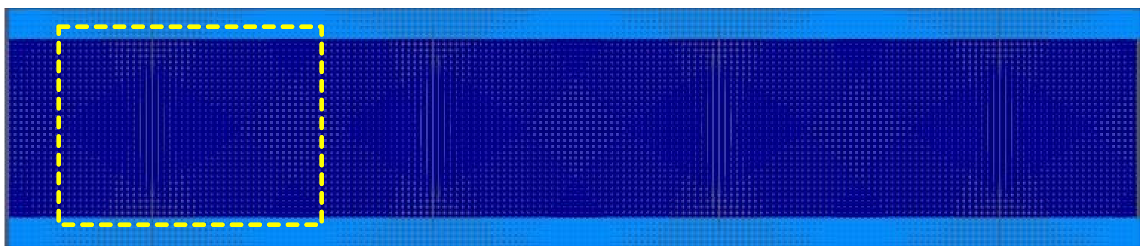

Asymmetric flame structure (w/o any treatments)

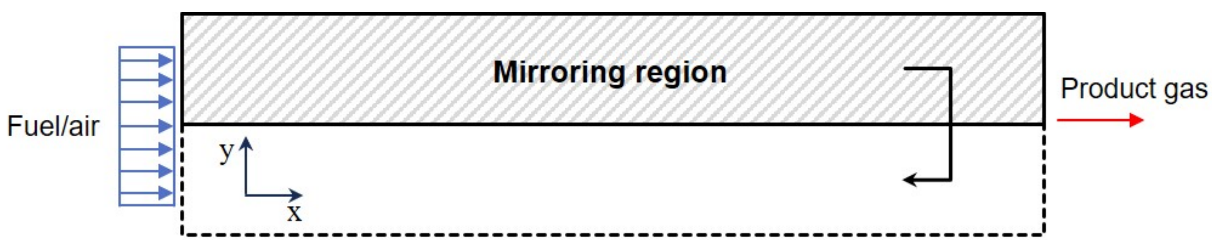

- The mirroring is performed in every 800-1,000 simulation counts which is found to give perfect symmetry with negligible computational loads.

Appendix F

- **Time-transient behavior of simulation results**

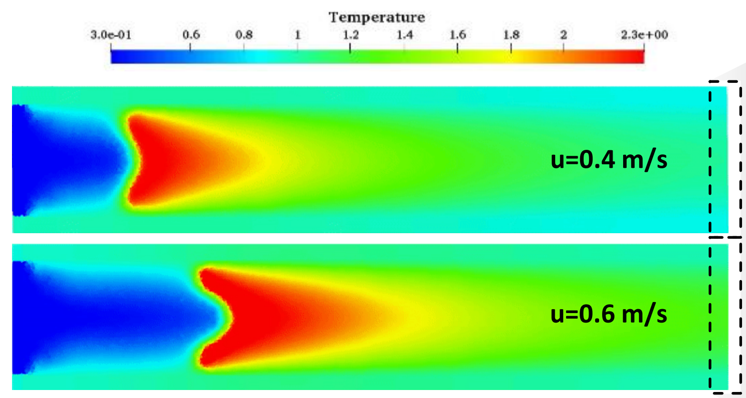

Transient motion of the flames

Pressure-outlet boundary

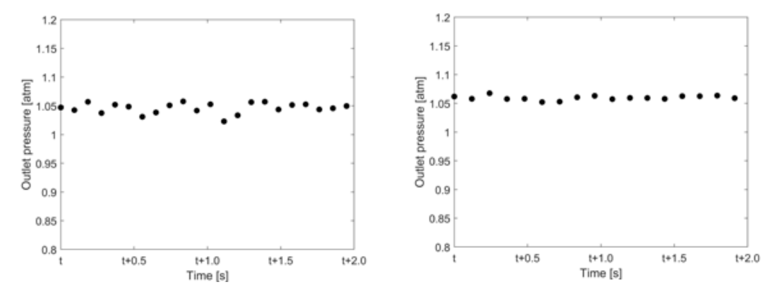

Outlet pressure with respect to time

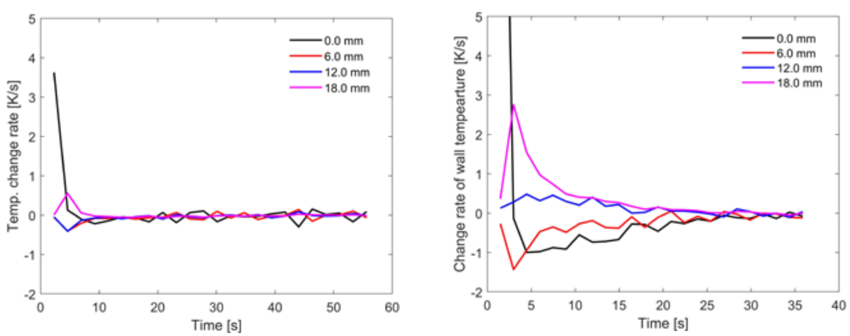

Wall temperature convergence at each location from the inlet

$$\frac{T^{n+1}(x) - T^{n}(x)}{\Delta t^{n}}$$

- Time average of $P_{f,outlet}$ is about 1.05 atm which meets pressure-outlet boundary condition at the exit well.
- Temperature of the combustor wall does converge even though the flames show the transient motion which is oscillatory within limited region inside the combustor.

Reference

1. Aikun Tang, Yiming Xu, Jianfeng Pan, Wenming Yang, Dongyue Jiang, Qingbo Lu, Combustion characteristics and performance evaluation of premixed methane/air with hydrogen addition in a micro-planar combustor, Chemical Engineering Science, Volume 131, 2015, Pages 235-242, ISSN 0009-2509,
2. Byung Ha PARK & Hee Cheon NO (2010) Strength Degradation of Oxidized Graphite Support Column in VHTR, Journal of Nuclear Science and Technology, 47:11, 998-1004
3. Chen, J., Liu, B., Gao, X., & Xu, D. (2016). Computational Fluid Dynamics Simulations of Lean Premixed Methane-Air Flame in a Micro-Channel Reactor Using Different Chemical Kinetics, *International Journal of Chemical Reactor Engineering*, *14*(5), 1003-1015.
4. Eung Soo Kim, Hee Cheon No, Byung Joon Kim, Chang H. Oh, Estimation of graphite density and mechanical strength variation of VHTR during air-ingress accident, Nuclear Engineering and Design, Volume 238, Issue 4, 2008, Pages 837-847
5. Fraser, Kirk & Kiss, Laszlo & St-George, Lyne. (2016). Adaptive Thermal Boundary Conditions for Smoothed Particle Hydrodynamics.
6. Fumihisa NAGASE & Toyoshi FUKETA (2006) Fracture Behavior of Irradiated Zircaloy-4 Cladding under Simulated LOCA Conditions, Journal of Nuclear Science and Technology, 43:9, 1114-1119
7. Gamma+ Volume II: Theory Manual (03/2017)
8. J.J. Monaghan, SPH without a tensile instability, J. Comput. Phys. 159 (2000) 290–311.
9. Liu, W.T., Sun, P.N., Ming, F.R. *et al.* Application of particle splitting method for both hydrostatic and hydrodynamic cases in SPH. *Acta Mech. Sin.* 34, 601–613 (2018).
10. Norton, D.G., Vlachos, D.G., 2003. Combustion characteristics and flame stability at the microscale: a CFD study of premixed methane/air mixtures. Chem. Eng. Sci. 58, 4871–4882.
11. Westbrook, C. K., & Dryer, F. L. (1981). Simplified reaction mechanisms for the oxidation of hydrocarbon fuels in flames. Combustion Science and Technology, 27, 31–43.